

1 **Lysine acetyltransferase Tip60 is required for hematopoietic stem cell maintenance**

2 Akihiko Numata,<sup>1\*</sup> Hui Si Kwok,<sup>1\*</sup> Qi-Ling Zhou,<sup>1\*</sup> Jia Li,<sup>1</sup> Roberto Tirado-Magallanes,<sup>1</sup> Vladimir  
3 Espinosa Angarcia,<sup>1</sup> Rebecca Hannah,<sup>2</sup> Jihye Park,<sup>3</sup> Chelsia Qiuxia Wang,<sup>1</sup> Vaidehi Krishnan,<sup>1</sup> Deepa  
4 Rajagopalan,<sup>1</sup> Yanzhou Zhang,<sup>1</sup> Siqin Zhou,<sup>1</sup> Robert S. Welner,<sup>4</sup> Motomi Osato,<sup>1</sup> Sudhakar Jha,<sup>1</sup> Stefan  
5 K. Bohlander,<sup>5</sup> Berthold Göttgens,<sup>2</sup> Henry Yang,<sup>1</sup> Touati Benoukraf,<sup>1</sup> John Lough,<sup>6</sup> Deepak Bararia,<sup>1,7\*\*</sup>  
6 and Daniel G. Tenen<sup>1,7\*\*</sup>

- 7  
8 1. Cancer Science Institute of Singapore, National University of Singapore, Singapore 117599,  
9 Singapore  
10 2. Department of Haematology, Wellcome and Medical Research Council Cambridge Stem Cell  
11 Institute & Cambridge Institute for Medical Research, Cambridge University, Cambridge, United  
12 Kingdom  
13 3. Department of Pathology, Beth Israel Deaconess Medical Center, Boston, USA  
14 4. Division of Hematology/Oncology, The University of Alabama at Birmingham, Comprehensive  
15 Cancer Center, Birmingham, USA  
16 5. Leukaemia and Blood Cancer Research Unit, Department of Molecular Medicine and Pathology,  
17 University of Auckland, Auckland, New Zealand  
18 6. Department of Cell Biology Neurobiology and Anatomy and the Cardiovascular Center, Medical  
19 College of Wisconsin, Milwaukee, USA  
20 7. Harvard Stem Cell Institute, Harvard Medical School, Boston, USA

21 \* Co-first authors.

22 \*\* Corresponding authors.

23  
24  
25 **§Contact:**

26 Daniel G. Tenen

27 Cancer Science Institute of Singapore, National University of Singapore

28 Centre for Translational Medicine, 14 Medical Drive, #12-01 North Core

29 Singapore 117599, Singapore

30 Tel: +65-6516-1159

31 FAX: +65-6873-9664

32 [daniel.tenen@nus.edu.sg](mailto:daniel.tenen@nus.edu.sg)

33 **Key points**

- 34 ▪ Conditional deletion of *lysine acetyltransferase 5 (Tip60)* in murine hematopoietic system leads to
- 35 HSC loss, both in fetal and adult stage.
- 36 ▪ **c-Myc is the most enriched transcription factor with genome-wide binding of Tip60 in murine**
- 37 **hematopoietic stem and progenitor cells.**
- 38 ▪ **Tip60 activates Myc target genes critical for HSC maintenance through acetylation of H2A.Z at the**
- 39 **target genomic regions.**

40

41 **Abstract**

42 Hematopoietic stem cells (HSC) have the potential to replenish the blood system for the lifetime of the  
43 organism. Their two defining properties, self-renewal and differentiation, are tightly regulated by the  
44 epigenetic machineries. Here, using conditional gene knockout models, we demonstrate a critical  
45 requirement of lysine acetyltransferase 5 (*Kat5*, also known as *Tip60*) for murine HSC maintenance both  
46 in the embryonic and adult stages, which depends on its acetyltransferase activity. Genome-wide  
47 chromatin and transcriptome profiling in murine hematopoietic stem and progenitor cells revealed that  
48 Tip60 co-localizes with c-Myc and that *Tip60* deletion suppress the expression of Myc target genes,  
49 which are associated with critical biological processes for HSC maintenance, cell-cycle and DNA repair.  
50 Notably, acetylated H2A.Z (acH2A.Z) was enriched at the Tip60-bound active chromatin and *Tip60*  
51 deletion induced a robust reduction in the acH2A.Z / H2A.Z ratio. These results uncover a critical  
52 epigenetic regulatory layer for HSC maintenance at least in part through Tip60 dependent H2A.Z  
53 acetylation to activate Myc target genes.

54

## 55 **Introduction**

56 Hematopoietic stem cells (HSCs) possess two defining properties, a self-renewal and multi-lineage  
57 differentiation ability, under various tightly regulated epigenetic mechanisms<sup>1</sup>. Chromatin modifying  
58 enzymes play crucial roles in regulating gene expression for HSC maintenance<sup>2-5</sup>. Histone acetylation, a  
59 reversible-covalent post-translational modification (PTM), is one of the most studied chromatin  
60 modifications, which is catalyzed by lysine acetyltransferases (KATs) and mediates unique and specific  
61 effects on gene transcription by altering the degree of chromatin condensation<sup>6,7</sup>. According to  
62 structural homology and acetylation mechanisms, KATs are classified into five representative families:  
63 GNAT, MYST, p300/CBP, SRC, and TAF1<sup>8</sup>. The MYST family is defined by the proteins containing a  
64 C<sub>2</sub>HC-type zinc finger and an acetyl-CoA binding domain, and consists of five members: *Tip60/Kat5*,  
65 *Moz/Kat6a*, *Morf/Kat6b*, *Hbo1/Kat7*, and *Mof/Kat8*. Previous studies of various KAT deletions in mice  
66 detailed their importance in the maintenance or differentiation of HSCs. Homozygous deletion and  
67 catalytic mutant mice of *Moz/Kat6a* revealed its essential role in both fetal and adult HSC maintenance  
68 as a repressor of p16 expression to prevent HSC senescence<sup>5,9</sup>. *Mof/Kat8* is critical for adult, not fetal  
69 HSC maintenance, and the catalytically inactive mutant neither restores H4K16ac levels nor rescues  
70 colony forming ability in adult hematopoiesis<sup>10</sup>. The Hbo1-Brd1 complex is required for transcription  
71 of genes regulating erythroid development<sup>11</sup>. Each lysine acetyltransferase has a specific regulatory role  
72 in hematopoiesis despite some redundancy in their substrate specificities<sup>12</sup>.

73 Lysine acetyltransferase 5, Kat5 (also known as Tat-Interactive Protein 60, Tip60) plays a key role in  
74 DNA damage response and repair, as well as gene-specific transcriptional regulation<sup>13</sup>. It is part of the  
75 evolutionarily conserved Nucleosomal Acetyltransferase of H4 (NuA4) protein complex, which  
76 acetylates nucleosomal histones H3, H4, H2A, and H2A variants<sup>14</sup>. Homozygous global *Tip60* deletion  
77 in mice lead to pre-implantation lethality at embryonic day 3.5<sup>15</sup>, indicating its requirement for

78 embryonic development. In the hematopoietic system, a conditional deletion of *Tip60* in regulatory T  
79 (Treg) cells impairs their function in peripheral immune organs by suppressing the transcriptional  
80 activity of FOXP3<sup>16</sup>. However, the role of Tip60 in HSCs has been largely unknown. Here, we  
81 demonstrate a critical requirement for *Tip60* in murine HSC maintenance using murine conditional  
82 *Tip60* deletion models. Genome-wide transcriptome and chromatin profiling reveal that Tip60 and c-  
83 Myc co-localize at active chromatin loci to activate transcription of their target genes. Notably, Tip60  
84 deletion reduces acetylation level of H2A.Z at the target genes promoters. We thus propose a new  
85 epigenetic mechanism in HSC maintenance: Tip60-mediated H2A.Z acetylation for the activation of  
86 Myc target genes.

## 87 **Materials and methods**

### 88 **Mice**

89 *Tip60<sup>lox</sup>* mice are generated by inserting *LoxP* sites flanking introns 2 and 11 of the mouse *Tip60* gene.  
90 Cre-recombinase-mediated excision was designed to remove exons 3 to 11, which includes the chromo-  
91 finger, zinc finger, and acetyl Co-A binding domains. Embryonic stem cell clones with correct  
92 homologous recombination were injected into *C57/Bl6* blastocysts, which transmitted the targeted allele  
93 via germline following implantation (supplemental Figures 1A-B). Additional details are described in  
94 the supplemental information. All mice were housed in a sterile barrier facility within the Comparative  
95 Medicine facility at the National University of Singapore. All mice experiments performed in this study  
96 were approved by Institutional Animal Care and Use Committee.

### 97 **Inducible *Tip60* deletion**

98 For *in vivo Tip60* deletion, *Mx1-cre; Tip60<sup>ff</sup>* mice were injected with 300 µg pIpC (GE Healthcare) per  
99 body for three consecutive days. For *in vitro Tip60* deletion, LSK or c-Kit<sup>+</sup> cells were sorted from fetal  
100 liver of *Rosa26 Cre-ERT2; Tip60<sup>ff</sup>* embryos (E13.5-15.5) by FACS Aria (BD Biosciences), cultured in  
101 Stemline II (Sigma-Aldrich) supplemented with 5% FBS, murine recombinant SCF 100ng/µL, IL-3 6  
102 ng/µL, IL-6 10ng/µL, IL-11 20 ng/µL (Peprotech), and 4-Hydroxytamoxifen (4-OHT) (Sigma-Aldrich)  
103 400 nM for 72 hours, and collected for analysis.

### 104 **Flow cytometry**

105 Single-cell suspensions were analyzed by flow cytometry. Cells stained with antibodies were analyzed  
106 or sorted using LSRII flow cytometer or FACS Aria (BD Biosciences). Flow Jo 7.5 (Tree Star) was used  
107 for data analysis. The antibodies used in this study are described in the supplemental information.

108 **Retroviral transduction and Tip60 KAT rescue**

109 FLAG-tagged human TIP60 wild-type and catalytically inactive mutant constructs<sup>17</sup> were cloned into  
110 MSCV vector (*TIP60<sup>wt</sup>* and *TIP60<sup>mut</sup>*, respectively). *TIP60<sup>wt</sup>* and *TIP60<sup>mut</sup>* retroviruses were produced in  
111 BOSC23 cells. FACS-sorted LSK cells obtained from *Tip60<sup>ff</sup>*; *Vav-iCre* embryos (CD45.2<sup>+</sup>) at E13.5  
112 were seeded in Retronectin (Takara)-coated plates containing retroviral supernatants for 24 hours.  $2 \times 10^3$   
113 transduced cells were injected into lethally (900 rads) irradiated congenic mice (CD45.1<sup>+</sup>) along with  
114 wild type WBM cells from congenic mice (CD45.1<sup>+</sup> CD45.2<sup>+</sup>). Transduction of plasmid DNAs were  
115 verified by Sanger sequencing of the PCR-amplified genomic products amplified by the following  
116 primers: Tip60KAT-F: 5'- GTG TTT CCT TGA CCA TAA GAC ACT GTA CTA T -3' and  
117 Tip60KAT-R: 5'- GGT CTG GGA CCA GTA GCT TCG ATA G -3'.

118 **Bone marrow transplantation assay**

119 For competitive transplantation assay, unfractionated fetal liver cells ( $1 \times 10^6$  cells) from *Tip60<sup>ff/+</sup>*,  
120 *Tip60<sup>+/-</sup>*, and *Tip60<sup>Δ/Δ</sup>* E14.5 embryos were injected into lethally irradiated (900 rads) congenic mice  
121 along with competitor WBM cells ( $1 \times 10^5$  cells). *Mx1-Cre*; *Tip60<sup>ff</sup>* and *Tip60<sup>ff</sup>* mice, which were  
122 injected 800 μg of pIpC per body every other day for 7 days, whole BM (WBM) cells ( $1 \times 10^6$  cells) were  
123 collected 10 days after the last injection, and then injected into lethally irradiated congenic mice along  
124 with competitor WBM cells ( $2 \times 10^5$  cells). For reciprocal transplantation assays, unfractionated WBM  
125 cells from *Mx1-Cre*; *Tip60<sup>ff</sup>* and *Tip60<sup>ff</sup>* mice were injected into lethally irradiated (900 rads) congenic  
126 mice along with competitor WBM cells ( $1 \times 10^6$  and  $2 \times 10^5$ ,  $5 \times 10^5$  and  $5 \times 10^5$  cells, respectively), and the  
127 recipients were injected with 800 μg of pIpC per body every other day for 4 days after engraftment. To  
128 exclude cell extrinsic effect caused by *Tip60* deletion, unfractionated CD45.1<sup>+</sup> WBM cells ( $1 \times 10^6$  cells)  
129 were injected into lethally irradiated *Tip60<sup>ff</sup>* and *Tip60<sup>ff</sup>*; *Mx1-Cre* mice. After transplantation,  
130 chimerism analysis was performed as described in the supplemental information.

131 **RNA/ChIP-sequencing**

132 RNA-seq libraries were prepared using Illumina Tru-Seq Stranded Total RNA with Ribo-Zero Gold kit  
133 protocol, according to the manufacturer's instructions (Illumina, San Diego, California, USA). Libraries  
134 were validated with an Agilent Bioanalyzer (Agilent Technologies, Palo Alto, CA), diluted and applied  
135 to an Illumina flow cell using the Illumina Cluster Station. ChIP-seq libraries were prepared using Next  
136 ChIP-Seq library prep reagent set and multiplexed (New England Biolabs). Each library was sequenced  
137 on an Illumina HiSeq2000 sequencer. The details of chromatin immunoprecipitation and sequence  
138 analysis are described in the supplemental information.

139 **ChIP-Seq similarity analysis**

140 Similarity analysis was performed using normalized pointwise mutual information (NPMI)<sup>18</sup>. After  
141 normalization, NPMI ranged from 1 for complete co-occurrence (correlation limit), 0 for independent  
142 peaks profiles, and -1 when peaks did not occur together (anticorrelation limit). NPMI values were  
143 clustered using Euclidean distance and Ward linkage in R. All data sets except Tip60 profiling are  
144 accessible through an intuitive Web browser interface (CODEX). <http://codex.stemcells.cam.ac.uk/>

145 **Statistical analysis**

146 The statistical significances were assessed by Student's unpaired t-test using the GraphPad software  
147 unless otherwise specified.

148 Additional details are described in the supplemental information.

149 **Data availability**

150 The RNA-seq and ChIP-seq data described in this study have been deposited in GEO under accession  
151 number GEO: GSE120705.

## 152 **Results**

### 153 **Tip60 deletion leads to rapid HSC loss in both fetal and adult stages**

154 To study the role of *Tip60* in HSCs, we generated mice in which a loxP-flanked *Tip60* allele (exons 3 to  
155 11, which includes the chromo, zinc finger and acetyl Co-A binding domains) (supplemental Figures  
156 1A-B)<sup>16</sup> was conditionally deleted by improved Cre (iCre) recombinase whose expression was under  
157 the control of the *Vav1* promoter (*Tip60<sup>ff</sup>; Vav-iCre*) (supplemental Figures 2A-C)<sup>19</sup>. *Tip60<sup>ff/+</sup>; Vav-iCre*  
158 and *Tip60<sup>ff/ff</sup>* mice were crossed, and among the 76 viable progenies obtained, none of the 19 (25%)  
159 expected *Tip60<sup>ff/ff</sup>; Vav-iCre* (*Tip60<sup>Δ/Δ</sup>*) mice were born (Figure 1A). In a retrospective analysis, *Tip60<sup>Δ/Δ</sup>*  
160 embryos were viable at E14.5, however, they became anemic at E17.5 (Figure 1B), suggesting that the  
161 cause of the lethality of *Tip60<sup>Δ/Δ</sup>* embryos was hematopoietic failure, mainly anemia (supplemental  
162 Figure 2D). *Tip60* deletion led to a decrease in the size of the fetal liver, accompanied by 6 to 9-fold  
163 reductions in the number of fetal liver cells at E14.5 and E17.5 (Figure 1C and supplemental Figure 2E).  
164 The subpopulations of hematopoietic stem and progenitor cells (HSPCs) were dramatically reduced  
165 (Figures 1D-E). To assess the repopulating ability, we performed competitive transplantation using  
166 whole fetal liver cells of E14.5 embryos, which demonstrated complete loss of hematopoietic  
167 reconstitution by *Tip60<sup>Δ/Δ</sup>* cells (Figure 1F and supplemental Figures 2F-G). There were few *Tip60<sup>Δ/Δ</sup>*  
168 HSCs present in the bone marrow (BM) of the recipients at 16 weeks post-transplantation, suggesting an  
169 impaired long-term repopulating ability of fetal *Tip60<sup>Δ/Δ</sup>* HSCs (Figure 1G). Notably, heterozygous  
170 deletion of *Tip60* (*Tip60<sup>+/-Δ</sup>*) did not affect hematopoietic reconstitution, which indicated that there was  
171 no gene dosage effect of *Tip60* in HSC function.

172 To determine the role of *Tip60* in adult HSCs, we generated *Tip60<sup>ff/ff</sup>* and *Tip60<sup>ff/+</sup>* mice wherein  
173 expression of Cre is driven by the interferon-inducible promoter of the gene encoding Mx1. In this



174 model, the *Tip60* gene was excised by injecting polyinosinic-polycytidylic acid (pIpC), leading to a  
175 reduction of Tip60 protein in HSPCs (supplemental Figures 3A-C)<sup>20</sup>. *Tip60* deletion induced a  
176 dramatic decrease in cellularity and numbers of HSPCs in BM (Figures 2A-B), whereas heterozygous  
177 *Tip60* deletion did not, again demonstrating the absence of a gene dosage effect of Tip60 in adult  
178 hematopoiesis as well. In competitive transplantations, *Tip60<sup>Δ/Δ</sup>* whole BM (WBM) cells did not  
179 reconstitute hematopoiesis (Figure 2C and supplemental Figure 3D), with few or no *Tip60<sup>Δ/Δ</sup>* HSCs were  
180 detected in the BM 16 weeks after the transplantation (Figure 2D), indicating an impaired long-term  
181 repopulating ability in adult stage as well. Short-term *in vivo* homing assays demonstrated no significant  
182 difference in engraftment efficiency (Figure 2E).

### 183 **Tip60 is a critical cell-intrinsic regulator of HSC**

184 Since Cre under Mx1 promoter is activated by pIpC in various tissues<sup>20</sup>, reciprocal competitive  
185 transplantations were conducted to exclude a cell-extrinsic effect of *Tip60* deletion. First, WBM cells  
186 from *Tip60<sup>ff</sup>; Mx1-Cre* or *Tip60<sup>ff</sup>* mice were transplanted into lethally irradiated congenic mice and  
187 pIpC was injected into the recipients 6 weeks post-transplantation. Peripheral blood (PB) chimerism  
188 analysis revealed a continuous decrease in *Tip60<sup>ff</sup>; Mx1-Cre* cells in all lineages over time, but not in  
189 control (*Tip60<sup>ff</sup>*) cells (Figure 2F and supplemental Figure 3E). Secondly, WBM cells from congenic  
190 mice were transplanted into lethally irradiated recipients, *Tip60<sup>ff</sup>; Mx1-Cre* and *Tip60<sup>ff</sup>* mice, which  
191 were subsequently injected with pIpC. The chimerism of donor-derived cells was sustained in both  
192 groups for 8 weeks. However, all the *Tip60<sup>ff</sup>; Mx1-Cre* recipients died within 3 months (supplemental  
193 Figure 3F) with clinical presentations of severe dermatitis, hair loss, and deteriorating general condition.  
194 PB analysis demonstrated stable blood counts, which were derived from donor mice (data not shown),  
195 suggesting that the hematopoietic defect was not the cause of death. Given that Tip60 plays a critical  
196 role in response to DNA double-strand breaks (DSBs)<sup>17, 21</sup>, *Tip60* deletion may have exacerbated the

197 genotoxicity of irradiation, leading to fatal failure of non-hematopoietic organs wherein *Tip60* is deleted.  
198 In summary, we conclude that Tip60 is a critical cell-intrinsic regulator for HSCs.

### 199 **Tip60 acetyltransferase activity is essential for HSC function**

200 Since our conditional deletion model ablates all the functional domains of Tip60, we investigated  
201 whether its acetyltransferase activity is required for HSC function. We overexpressed both wild-type  
202 TIP60 and acetyltransferase defective TIP60 (Q377E/G380E)<sup>17</sup> in HEK293T cells and confirmed that  
203 both proteins were expressed at similar levels (supplemental Figure 4A). *Tip60<sup>Δ/Δ</sup>* LSK cells purified  
204 from E13.5 fetal livers were transduced with retroviruses expressing wild-type TIP60 (TIP60<sup>wt</sup>),  
205 TIP60<sup>mut</sup>, or empty vector (Empty) and subsequently transplanted into lethally irradiated congenic mice  
206 along with wild-type WBM cells (Figure 3A and supplemental Figure 4B). The *Tip60<sup>Δ/Δ</sup>* LSK cells  
207 transduced with empty vector did not recover long-term hematopoiesis, while Tip60<sup>wt</sup> rescued the defect  
208 successfully (Figure 3B). Notably, the transduction of TIP60<sup>mut</sup> did not rescue the defect to any  
209 detectable level. Furthermore, we confirmed that both TIP60 wild-type and mutant could interact with  
210 key components of the NuA4 complex, including p400, RUVBL1, RUVBL2, and TRRAP  
211 (supplemental Figures 4C-E), suggesting that the catalytic mutations in TIP60 did not affect its binding  
212 to the complex. However, we cannot fully exclude the possibility that the TIP60 mutant could have  
213 some loss or gain of additional protein interactions that may account for its inability to rescue HSC  
214 regenerative capacity. Collectively, these results demonstrate a specific requirement of Tip60  
215 acetyltransferase activity for HSCs regenerative ability.

### 216 **Tip60 maintains HSC genome integrity**

217 To elucidate the cellular mechanisms underlying the loss of *Tip60<sup>Δ/Δ</sup>* HSCs, we assessed apoptosis and  
218 cell-cycle status. *Tip60* deletion induced apoptosis in fetal CD45<sup>+</sup> cells and adult HSCs, exhibiting

219 increased AnnexinV<sup>+</sup>DAPI<sup>-</sup> cells and cleaved caspase-3 levels (Figures 4A-B). Cell-cycle analysis  
220 revealed fewer quiescent *Tip60<sup>Δ/Δ</sup>* HSCs (G<sub>0</sub>: Ki67<sup>-</sup>Hoeschst<sup>-</sup>) with a concordant increased percentage of  
221 cells in cycling phase (S-G<sub>2</sub>/M: Ki67<sup>+</sup>Hoeschst<sup>+</sup>) compared to control (Figure 4C). Moreover, DNA  
222 content analysis, using fetal LSK cells of *Tip60<sup>ff</sup>; Rosa26-CreERT2* and *Tip60<sup>ff</sup>* embryos at E14.5,  
223 subsequently treated with 4-hydroxytamoxifen (4-OHT) in culture for 5 days, revealed an increase in  
224 cells with 4N or greater than 4N DNA content (Figure 4D). Such increase was not seen in LSK cells  
225 from *Rosa26-CreERT2* embryos, suggesting that this effect is specific to the deletion of *Tip60*  
226 (supplemental Figure 4F). Microscopic examination revealed that *Tip60<sup>Δ/Δ</sup>* cells grew in size and became  
227 multi-nucleated, exhibiting abnormal nuclear morphology including multi-lobulated nuclei and  
228 micronuclei (supplemental Figure 4G). Given that the Tip60 complex has been shown to be important  
229 for DNA double-stranded breaks (DSBs) repair process<sup>17, 21</sup>, we investigated DNA damage in *Tip60<sup>Δ/Δ</sup>*  
230 HSCs. Remarkably, alkaline comet assay demonstrated increased tail moment in *Tip60<sup>Δ/Δ</sup>* HSPCs  
231 (Figure 4E), suggesting that *Tip60* deletion impaired DNA repair, which was further verified by the  
232 accumulation of γH2AX signals, a marker for unrepaired DSB loci (Figure 4F). Collectively, these  
233 results indicate that *Tip60* deletion induces aberrant cell-cycle progression, and apoptosis that is possibly  
234 caused by DNA breaks in HSCs.

### 235 **Tip60 is required for expression of Myc target genes**

236 To identify genes regulated by Tip60 in a cell-intrinsic manner, we performed RNA-seq using LSK cells  
237 purified from *Tip60<sup>ff</sup>; Rosa26-CreERT2* and *Tip60<sup>ff</sup>* embryos that were treated with 4-OHT for 72 hours  
238 (supplemental Figures 5A-B). A total of 1,278 genes exhibited significant change in expression levels,  
239 with 847 genes up-regulated and 431 genes down-regulated (Log<sub>2</sub> fold change > 0.5 and false discovery  
240 rate (FDR) < 0.05) in *Tip60<sup>Δ/Δ</sup>* cells compared to control (*Tip60<sup>ff</sup>*) (supplemental Figure 5C). Gene set

241 enrichment analysis (GSEA) using Molecular Signature Database (MSigDB) revealed that E2f and Myc  
242 target genes were down-regulated in *Tip60<sup>Δ/Δ</sup>* cells (supplemental Figure 5D). Given that Tip60  
243 functions mainly as a transcriptional co-activator for several sequence-specific transcription factors<sup>22-24</sup>,  
244 it is plausible that a variety of transcription factors are involved in the underlying mechanisms for the  
245 rapid loss of *Tip60<sup>Δ/Δ</sup>* HSCs. Hence, an open-ended GSEA was conducted using all available gene sets of  
246 transcription factor targets. Interestingly, multiple Myc-associated gene sets were specifically enriched  
247 in control (Figures 5A-B). While c-Myc at RNA and protein levels were not suppressed (supplemental  
248 Figures 5E, F), most Myc target genes were transcriptionally inactivated upon *Tip60* deletion. Among  
249 the 124 differentially expressed Myc target genes (supplemental Figure 5G), we observed a significant  
250 over-representation of Tip60 targets in the downregulated group compared to the upregulated group (*p*-  
251 value < 10<sup>-5</sup>; Fisher's exact test) (supplemental Figure 5H). Our results demonstrate that Tip60 acts as a  
252 co-activator of Myc target genes.

253 Cell-cycle regulators play a pivotal role in HSC maintenance by tuning the balance between quiescence  
254 and self-renewal<sup>25</sup>. The DNA repair process is critical as well, exemplified by the recent studies which  
255 demonstrated that HSCs are susceptible to DNA damage due to intrinsic and extrinsic stress factors,  
256 such as aging, replication, and genotoxic and oxidative stresses<sup>26-28</sup>. Of note, the genes which were  
257 inactivated by *Tip60* deletion are associated with cell-cycle and DNA repair. Therefore, we conclude  
258 that Tip60 maintains HSC functional integrity, mainly cooperating with Myc family transcription factors  
259 to activate the multiple genes which are involved in essential cellular processes for HSC maintenance.

### 260 **Tip60 and Myc co-activate target genes**

261 To better understand the involvement of Tip60 in the active transcription of Myc target genes, we  
262 performed genome-wide ChIP-seq assays in the murine hematopoietic progenitor cell line HPC-7<sup>29</sup>,

263 using rabbit polyclonal antibodies that specifically recognize endogenous Tip60<sup>23</sup>. The majority of 4347  
264 of high-confidence Tip60-bound genomic loci identified were located at the proximal promoter regions  
265 (-1kb, +100bp from transcriptional start sites; TSS, 66.7 %), including the promoters of previously  
266 reported Tip60 target genes (*Ncl*, *Rps9*, and *Cdkn1b*)<sup>23, 30, 31</sup> (supplemental Figures 6A-B). To define the  
267 transcription factors that Tip60 co-localizes with, a correlation analysis of genome-wide Tip60 and 10  
268 hematopoietic transcription factors (c-Myc, Tal1, Gata2, Lyl1, Lmo2, Runx1, Fli1, Meis1, Gfi1b, and  
269 Spi1) occupancy was performed as previously described<sup>18</sup>. Notably, c-Myc was the most enriched  
270 transcription factor in the Tip60-bound regions (Figure 5C), which corroborates the findings from our  
271 RNA-seq analysis. Given that Myc binding peaks are not more than those of other transcription factors,  
272 a specificity of Tip60 co-localization with c-Myc does not reflect abundance of c-Myc binding peaks.  
273 Co-localization of c-Myc and Tip60 at the promoters of the target genes was validated by ChIP-qPCR  
274 (supplemental Figure 6C). Consistent with previous studies in non-hematopoietic cells<sup>23</sup>, we  
275 demonstrated that Tip60 interacts with c-Myc by reciprocal co-immunoprecipitation experiments in  
276 murine hematopoietic progenitor cells, 32D (Figure 5D).

277 To delineate the chromatin conformations, we generated heatmaps of ChIP-seq peak signals  
278 between -4 kb to 4 kb from TSS region for Tip60, active promoter histone mark H3K4me3, repressive  
279 histone mark H3K27me3, and DNase 1 hypersensitive sites (DHSs)<sup>18</sup>, and ranked the gene order based  
280 on RNA expression levels (supplemental Figure 6D). Remarkably, the Tip60 binding intensity  
281 correlated with the RNA levels of the corresponding genes, and its occupancy overlapped with an  
282 H3K4me3 enrichment and DHSs, but not with the H3K27me3. Given that c-Myc and N-myc bind  
283 specifically to a common consensus sequence<sup>32, 33</sup>, we conclude that Tip60 co-localizes with Myc  
284 proteins at the transcriptional regulatory elements and active chromatin regions to activate genes in  
285 HSPCs.

## 286 **Tip60 maintains acetylated H2A.Z at Myc target genes**

287 Tip60 has been demonstrated to acetylate histones H3, H4, H2A, and H2A variants as well as non-  
288 histone proteins<sup>13,17</sup>. H2A.Z is an evolutionarily conserved variant of the canonical H2A. In  
289 *Saccharomyces cerevisiae*, ESA1, the yeast ortholog of Tip60, also mediates the acetylation of Htz1, the  
290 ortholog of H2A.Z<sup>34,35</sup>. *Drosophila* Tip60 acetylates lysine 5 of H2Av, a functional homolog of the  
291 mammalian H2A.Z isoform<sup>36</sup>. H2A.Z is enriched around TSS across the different species<sup>37,38</sup>, whereas  
292 an acetylated form of H2A.Z (acH2A.Z) is enriched at active promoter region<sup>39</sup> and confers nucleosome  
293 destabilization and open chromatin conformation<sup>40</sup>. **We evaluated global histone acetylation levels upon**  
294 **overexpression of Tip60 in the hematopoietic progenitor cells 32D and found an increased H2A.Z**  
295 **acetylation levels as well as H4K16, known histone substrate of Tip60 (Supplemental Figure 7A). Given**  
296 **that H2A.Z has been linked with actively transcribed regions, we further evaluated the changes in**  
297 **acH2A.Z along with an active enhancer and promoter mark (H3K27ac) and a repressive mark**  
298 **(H3K27me3), evoked by *Tip60* deletion by performing ChIP-seq (supplemental Figure 7B).** Consistent  
299 with the findings from a previous study<sup>41</sup>, both acH2A.Z and H2A.Z were enriched at the active  
300 chromatin marked by H3K27ac (Figure 6A), and acH2A.Z exhibited a pronounced bimodal enrichment  
301 around TSS at highly expressed genes, while exhibiting less enrichment at poorly expressed genes and  
302 no enrichment at untranscribed genes (supplemental Figure 7C). Remarkably, we observed that the  
303 transcription levels for genes which were highly enriched in acH2A.Z and H2A.Z marks around TSS are  
304 significantly higher than all transcribed genes (supplemental Figure 7D). We also observe a similar trend  
305 for genes with H3K27ac enrichment, whereas those with H3K27me3 marks exhibit a significant  
306 decrease in their transcription levels. Moreover, the ratio of acH2A.Z/H2A.Z around TSS correlated  
307 with RNA levels of the corresponding genes (Pearson correlation  $R^2=0.7$ ), and most of the Tip60-bound  
308 genes (82.0%) were highly expressed and had a higher acH2A.Z/H2A.Z ratio (Figure 6B).

309 Notably, *Tip60* loss reduced acH2A.Z levels at the promoters of the *Tip60*-bound *Myc* genes and  
310 the *Tip60*-bound distal regions, whereas neither H3K27ac nor H3K27me3 enrichment levels were  
311 altered (Figure 6C and supplemental Figure 7E). H2A.Z abundance within nucleosomes at *Tip60*-bound  
312 promoters was not decreased; indicating that reduced acetylation of H2A.Z is not a direct consequence  
313 of H2A.Z eviction. *Myc* target genes (816 genes), which we obtained from *Myc*-associated gene sets  
314 (Figure 5A), demonstrated reduced acH2A.Z/H2A.Z ratios around TSS and significant downregulation  
315 of their RNA levels (217 genes), including various genes related to cell-cycle and DNA repair (Figure  
316 6D and supplemental Figure 7F). We conducted additional analysis for *Tal1* and *PU.1* (*Spi-1*) target  
317 genes obtained from public database (supplemental Figure 7G). We chose *Tal1* as a representative of the  
318 genes that showed minimum correlation with *Tip60* in the genome-wide occupancy analysis and *PU.1*  
319 (*Spi-1*) as a representative of genes that showed high correlation (supplemental Figure 5C). A higher  
320 proportion of *Myc* target genes (69.8%) exhibited decreased acH2AZ/H2AZ ratio and RNA expression  
321 compared to *Tal1* (33.02%) and *PU.1* target genes (28.47%). We thus propose that the *Tip60*-acH2A.Z  
322 epigenetic axis contributes to HSC survival through activation of *Myc* target genes (Figure 6E).

323 **Discussion**

324 The lysine acetyltransferase Tip60 is the catalytic subunit of the multiprotein complex NuA4 and acts  
325 mainly in this large molecular complex. Previous studies revealed a critical requirement for three  
326 subunits of the complex in normal hematopoiesis; ablation of the gene encoding E1A-binding protein  
327 p400<sup>42</sup>, transformation/transcription domain-associated protein (Trrap)<sup>43</sup>, and RuvB-like AAA ATPase  
328 1 (Ruvb11)<sup>44</sup>, resulted in rapid loss of adult HSCs from BM due to apoptosis. These subunits are  
329 required for the complex integrity, assembly and activity<sup>45-48</sup>, suggesting that the NuA4 complex is  
330 important for HSC maintenance. However, the role of Tip60, specifically the catalytic function, in  
331 normal hematopoiesis remains undefined. In the present study, we established *Tip60* conditional  
332 knockout mice in two different Cre strains (Vav-iCre and the Mx1-Cre) to study the role of Tip60 in  
333 both fetal and adult hematopoiesis. Importantly, we demonstrated that the acetyltransferase activity of  
334 Tip60 is critical for long-term regenerating ability of murine HSCs.

335 The conditional deletion of *Tip60* in murine hematopoietic cells evoked catastrophic DNA damage in  
336 HSCs at both fetal and adult stages, thereby resulting in rapid apoptosis. It is noteworthy that conditional  
337 deletion of *Tip60* in Treg cells increased their number in the thymus, while they were decreased in both  
338 the spleen and the lymph nodes<sup>16</sup>. These results highlight that loss of Tip60 does not always result in  
339 cell lethality. Given that recent studies employing DNA repair-deficient mouse models indicate that  
340 HSCs are vulnerable to intrinsic and extrinsic DNA damage<sup>26-28</sup>, *Tip60* deletion provoked apoptosis in  
341 HSCs due to cellular susceptibility to DNA damage. Therefore, the essentiality of Tip60 for cell survival  
342 could be cell context-dependent.

343 Tip60 deletion had a clear impact on functional HSCs loss. All the transplantation assays in this study  
344 were followed up at least for 16 weeks, thus excluding contribution from progenitor cells-derived



345 hematopoiesis. Indeed, bulk RNA-seq was performed using hematopoietic stem and progenitor cells,  
346 therefore, it is a possibility that gene expression changes in Myc and E2F targets could be a consequence  
347 of decreased number of proliferating cells. Nonetheless, the specific co-binding of Tip60 and Myc on  
348 the target gene promoters demonstrated by ChIP-seq analysis provides evidence for a direct role of  
349 Tip60 in the regulation of c-Myc target genes. Intriguingly, *Tip60* deletion did not suppress c-Myc RNA  
350 and protein levels, indicating that down-regulation of Myc target genes by Tip60 deletion is not a direct  
351 consequence of c-Myc levels. In line with a previous study<sup>23</sup>, we also demonstrated interaction of Tip60  
352 and c-Myc in hematopoietic progenitor cells. These results provide substantial evidence for a direct role  
353 of Tip60 in the regulation of Myc target genes. Noting that the HSC phenotype evoked by simultaneous  
354 *c-Myc* and *N-myc* deletion in a previous study<sup>49</sup> resembles those of the *Tip60* conditional knockout mice,  
355 we conclude that Tip60 maintains HSC survival by interacting with c-Myc to co-activate target genes.

356 We demonstrated that the catalytically inactive TIP60 mutant was not able to rescue the impaired HSC  
357 function although it maintained critical components of NuA4 complex, indicating that Tip60  
358 acetyltransferase activity was specifically required. H2A.Z has been validated to be a substrate of Tip60  
359<sup>34-36</sup>, and has various functions in different species, including gene activation and repression, DNA  
360 repair, heterochromatin formation, and chromosome segregation<sup>50-52</sup>. The diverse functions are  
361 influenced by PTMs, including acetylation, SUMOylation, ubiquitination, and methylation of lysines<sup>53</sup>.  
362 Among them, acetylation is the most studied PTM as active enhancer and promoter marks<sup>39, 40, 54, 55</sup>. We  
363 extended these findings to murine HSPCs by performing genome-wide ChIP-seq analysis to investigate  
364 how Tip60 impacts H2A.Z acetylation and chromatin structure. Notably, *Tip60* deletion resulted in a  
365 global reduction in acH2A.Z / H2A.Z ratio around TSSs as well as to some extent in distal enhancer  
366 regions of the Tip60-bound genes, and reduced expression of a portion of these corresponding genes,  
367 particularly *Myc* targets. These data indicate that Tip60-mediated H2A.Z acetylation may serve as a

368 prerequisite for active gene transcription although how acetylated H2A.Z facilitates this machinery has  
369 remained largely enigmatic. Tip60 has also been described to acetylate H3, H4 and non-histone proteins  
370 besides H2A.Z<sup>13</sup>. Additional targets besides H2A.Z may be involved in the regulation of genes for HSC  
371 survival, and therefore further work is necessary to study the detailed mechanisms.

372 Additionally, we cannot exclude the possibility that Tip60-acH2A.Z epigenetic axis may involve  
373 other transcription factors besides c-Myc. Recent studies have suggested a putative association between  
374 H2A.Z and transcription factor E2F1 and co-activator Brd2 in active gene transcription<sup>56,57</sup>. It will be of  
375 future interest to identify and investigate how Tip60 cooperates with different transcription factors to  
376 facilitate gene transcription through acetylation of H2A.Z. In summary, our study highlights the  
377 importance of Tip60 in maintaining proper cell-cycle progression and DNA repair in murine HSCs at  
378 both fetal and adult stages, which is at least in part mediated through Tip60-dependent acetylation of  
379 H2A.Z to activate Myc target genes.

## 380 **Acknowledgments**

381 This research is supported by the National Research Foundation Singapore and the Singapore Ministry  
382 of Education, Singapore Translational Research Award from the Singapore National Medical Research  
383 Council (NMRC/STaR/00018/2013 to DGT), NIH grants (R35CA197697 and P01HL131477 to DGT),  
384 Cancer Research UK (C1163/A21762 to BG) and the Wellcome Trust (206328/Z/17/Z to BG). SKB is  
385 supported by Leukaemia & Blood Cancer New Zealand and the family of Marijanna Kumerich. We  
386 would like to thank Bruno Amati (Italian Institute of Technology) for providing rabbit polyclonal Tip60  
387 antibodies, and Chunaram Choudhary (The Novo Nordisk Foundation Center for Protein Research) for  
388 helpful discussion. We thank Celestina Chin Ai Qi (Cancer Science Institute of Singapore) for  
389 proofreading of the manuscript, members of the Tenen laboratory and CSI Singapore for many helpful

390 discussions and technical support, and CSI FACS facility, Beijing Genomics Institute (Hong Kong) and  
391 Duke-NUS Genome Biology Facility (Singapore) for technical support.

392 **Authorship contributions**

393 Conceptualization, AN, SKB, JL, DB, and DGT; Methodology, AN, HSK, QZ, YZ, VK, MO, and DB;  
394 Formal Analysis, AN, HSK, QZ, JL, VEA, RH, SZ, RTM, CQW, and JP; Investigation, AN, HSK, TB,  
395 RSW, and DB; Resources, DR, SJ, BG and JL; Writing – Original Draft, AN and HSK; Writing –  
396 Review & Editing, AN, HSK, DB, and DGT; Visualization, AN, HSK, QZ and VEA; Supervision, DGT,  
397 Funding Acquisition, DGT.

398 **Disclosure of Conflicts of Interest**

399 The authors declared no competing no financial interests.

400 **Reference**

- 401 1. Orkin SH, Zon LI. Hematopoiesis: an evolving paradigm for stem cell biology. *Cell*. 2008;132(4):631-  
402 644.
- 403 2. Sharma S, Gurudutta G. Epigenetic Regulation of Hematopoietic Stem Cells. *Int J Stem Cells*.  
404 2016;9(1):36-43.
- 405 3. Konuma T, Oguro H, Iwama A. Role of the polycomb group proteins in hematopoietic stem cells. *Dev*  
406 *Growth Differ*. 2010;52(6):505-516.
- 407 4. Cullen SM, Mayle A, Rossi L, et al. Hematopoietic stem cell development: an epigenetic journey. *Curr*  
408 *Top Dev Biol*. 2014;107:39-75.
- 409 5. Katsumoto T, Aikawa Y, Iwama A, et al. MOZ is essential for maintenance of hematopoietic stem cells.  
410 *Genes Dev*. 2006;20(10):1321-1330.
- 411 6. Brownell JE, Zhou J, Ranalli T, et al. Tetrahymena histone acetyltransferase A: a homolog to yeast Gcn5p  
412 linking histone acetylation to gene activation. *Cell*. 1996;84(6):843-851.
- 413 7. Turner BM, Birley AJ, Lavender J. Histone H4 isoforms acetylated at specific lysine residues define  
414 individual chromosomes and chromatin domains in *Drosophila* polytene nuclei. *Cell*. 1992;69(2):375-384.
- 415 8. Arrowsmith CH, Bountra C, Fish PV, et al. Epigenetic protein families: a new frontier for drug discovery.  
416 *Nat Rev Drug Discov*. 2012;11(5):384-400.
- 417 9. Perez-Campo FM, Costa G, Lie ALM, et al. MOZ-mediated repression of p16(INK) (4) (a) is critical for  
418 the self-renewal of neural and hematopoietic stem cells. *Stem Cells*. 2014;32(6):1591-1601.
- 419 10. Valerio DG, Xu H, Eisold ME, et al. Histone acetyltransferase activity of MOF is required for adult but  
420 not early fetal hematopoiesis in mice. *Blood*. 2017;129(1):48-59.
- 421 11. Mishima Y, Miyagi S, Saraya A, et al. The Hbo1-Brd1/Brpf2 complex is responsible for global  
422 acetylation of H3K14 and required for fetal liver erythropoiesis. *Blood*. 2011;118(9):2443-2453.
- 423 12. Roth SY, Denu JM, Allis CD. Histone acetyltransferases. *Annu Rev Biochem*. 2001;70:81-120.
- 424 13. Squatrito M, Gorrini C, Amati B. Tip60 in DNA damage response and growth control: many tricks in one  
425 HAT. *Trends Cell Biol*. 2006;16(9):433-442.
- 426 14. Doyon Y, Cote J. The highly conserved and multifunctional NuA4 HAT complex. *Curr Opin Genet Dev*.  
427 2004;14(2):147-154.
- 428 15. Hu Y, Fisher JB, Koprowski S, et al. Homozygous disruption of the Tip60 gene causes early embryonic  
429 lethality. *Dev Dyn*. 2009;238(11):2912-2921.
- 430 16. Xiao Y, Nagai Y, Deng G, et al. Dynamic interactions between TIP60 and p300 regulate FOXP3 function  
431 through a structural switch defined by a single lysine on TIP60. *Cell Rep*. 2014;7(5):1471-1480.
- 432 17. Ikura T, Ogryzko VV, Grigoriev M, et al. Involvement of the TIP60 histone acetylase complex in DNA  
433 repair and apoptosis. *Cell*. 2000;102(4):463-473.
- 434 18. Wilson NK, Schoenfelder S, Hannah R, et al. Integrated genome-scale analysis of the transcriptional  
435 regulatory landscape in a blood stem/progenitor cell model. *Blood*. 2016;127(13):e12-23.
- 436 19. de Boer J, Williams A, Skavdis G, et al. Transgenic mice with hematopoietic and lymphoid specific  
437 expression of Cre. *Eur J Immunol*. 2003;33(2):314-325.
- 438 20. Kuhn R, Schwenk F, Aguet M, et al. Inducible gene targeting in mice. *Science*. 1995;269(5229):1427-  
439 1429.
- 440 21. Murr R, Loizou JI, Yang YG, et al. Histone acetylation by Trrap-Tip60 modulates loading of repair  
441 proteins and repair of DNA double-strand breaks. *Nat Cell Biol*. 2006;8(1):91-99.
- 442 22. Bararia D, Trivedi AK, Zada AA, et al. Proteomic identification of the MYST domain histone  
443 acetyltransferase TIP60 (HTATIP) as a co-activator of the myeloid transcription factor C/EBPalpha. *Leukemia*.  
444 2008;22(4):800-807.
- 445 23. Frank SR, Parisi T, Taubert S, et al. MYC recruits the TIP60 histone acetyltransferase complex to  
446 chromatin. *EMBO Rep*. 2003;4(6):575-580.
- 447 24. Legube G, Linares LK, Tyteca S, et al. Role of the histone acetyl transferase Tip60 in the p53 pathway. *J*  
448 *Biol Chem*. 2004;279(43):44825-44833.

- 449 25. Rossi L, Lin KK, Boles NC, et al. Less is more: unveiling the functional core of hematopoietic stem cells  
450 through knockout mice. *Cell Stem Cell*. 2012;11(3):302-317.
- 451 26. Beerman I, Seita J, Inlay MA, et al. Quiescent hematopoietic stem cells accumulate DNA damage during  
452 aging that is repaired upon entry into cell cycle. *Cell Stem Cell*. 2014;15(1):37-50.
- 453 27. Rossi DJ, Bryder D, Seita J, et al. Deficiencies in DNA damage repair limit the function of  
454 haematopoietic stem cells with age. *Nature*. 2007;447(7145):725-729.
- 455 28. Walter D, Lier A, Geiselhart A, et al. Exit from dormancy provokes DNA-damage-induced attrition in  
456 haematopoietic stem cells. *Nature*. 2015;520(7548):549-552.
- 457 29. Pinto do OP, Kolterud A, Carlsson L. Expression of the LIM-homeobox gene LH2 generates  
458 immortalized steel factor-dependent multipotent hematopoietic precursors. *EMBO J*. 1998;17(19):5744-5756.
- 459 30. Fazio TG, Huff JT, Panning B. An RNAi screen of chromatin proteins identifies Tip60-p400 as a  
460 regulator of embryonic stem cell identity. *Cell*. 2008;134(1):162-174.
- 461 31. Park JH, Sun XJ, Roeder RG. The SANT domain of p400 ATPase represses acetyltransferase activity and  
462 coactivator function of TIP60 in basal p21 gene expression. *Mol Cell Biol*. 2010;30(11):2750-2761.
- 463 32. Blackwell TK, Kretzner L, Blackwood EM, et al. Sequence-specific DNA binding by the c-Myc protein.  
464 *Science*. 1990;250(4984):1149-1151.
- 465 33. Ma A, Moroy T, Collum R, et al. DNA binding by N- and L-Myc proteins. *Oncogene*. 1993;8(4):1093-  
466 1098.
- 467 34. Babiarz JE, Halley JE, Rine J. Telomeric heterochromatin boundaries require NuA4-dependent  
468 acetylation of histone variant H2A.Z in *Saccharomyces cerevisiae*. *Genes Dev*. 2006;20(6):700-710.
- 469 35. Keogh MC, Mennella TA, Sawa C, et al. The *Saccharomyces cerevisiae* histone H2A variant Htz1 is  
470 acetylated by NuA4. *Genes Dev*. 2006;20(6):660-665.
- 471 36. Kusch T, Florens L, Macdonald WH, et al. Acetylation by Tip60 is required for selective histone variant  
472 exchange at DNA lesions. *Science*. 2004;306(5704):2084-2087.
- 473 37. Creighton MP, Markoulaki S, Levine SS, et al. H2AZ is enriched at polycomb complex target genes in  
474 ES cells and is necessary for lineage commitment. *Cell*. 2008;135(4):649-661.
- 475 38. Raisner RM, Hartley PD, Meneghini MD, et al. Histone variant H2A.Z marks the 5' ends of both active  
476 and inactive genes in euchromatin. *Cell*. 2005;123(2):233-248.
- 477 39. Valdes-Mora F, Song JZ, Statham AL, et al. Acetylation of H2A.Z is a key epigenetic modification  
478 associated with gene deregulation and epigenetic remodeling in cancer. *Genome Res*. 2012;22(2):307-321.
- 479 40. Ishibashi T, Dryhurst D, Rose KL, et al. Acetylation of vertebrate H2A.Z and its effect on the structure of  
480 the nucleosome. *Biochemistry*. 2009;48(22):5007-5017.
- 481 41. Barski A, Cuddapah S, Cui K, et al. High-resolution profiling of histone methylations in the human  
482 genome. *Cell*. 2007;129(4):823-837.
- 483 42. Fujii T, Ueda T, Nagata S, et al. Essential role of p400/mDomino chromatin-remodeling ATPase in bone  
484 marrow hematopoiesis and cell-cycle progression. *J Biol Chem*. 2010;285(39):30214-30223.
- 485 43. Loizou JI, Oser G, Shukla V, et al. Histone acetyltransferase cofactor Trrap is essential for maintaining  
486 the hematopoietic stem/progenitor cell pool. *J Immunol*. 2009;183(10):6422-6431.
- 487 44. Bereshchenko O, Mancini E, Luciani L, et al. Pontin is essential for murine hematopoietic stem cell  
488 survival. *Haematologica*. 2012;97(9):1291-1294.
- 489 45. Auger A, Galarneau L, Altaf M, et al. Eaf1 is the platform for NuA4 molecular assembly that  
490 evolutionarily links chromatin acetylation to ATP-dependent exchange of histone H2A variants. *Mol Cell Biol*.  
491 2008;28(7):2257-2270.
- 492 46. Elias-Villalobos A, Toullec D, Faux C, et al. Chaperone-mediated ordered assembly of the SAGA and  
493 NuA4 transcription co-activator complexes in yeast. *Nat Commun*. 2019;10(1):5237.
- 494 47. Mitchell L, Lambert JP, Gerdes M, et al. Functional dissection of the NuA4 histone acetyltransferase  
495 reveals its role as a genetic hub and that Eaf1 is essential for complex integrity. *Mol Cell Biol*. 2008;28(7):2244-  
496 2256.
- 497 48. Jha S, Gupta A, Dar A, et al. RVBs are required for assembling a functional TIP60 complex. *Mol Cell*  
498 *Biol*. 2013;33(6):1164-1174.

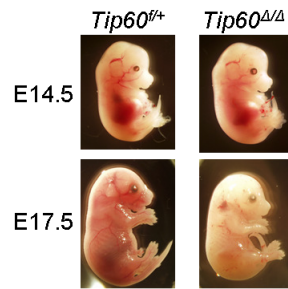
- 499 49. Laurenti E, Varnum-Finney B, Wilson A, et al. Hematopoietic stem cell function and survival depend on  
500 c-Myc and N-Myc activity. *Cell Stem Cell*. 2008;3(6):611-624.
- 501 50. Altaf M, Auger A, Covic M, et al. Connection between histone H2A variants and chromatin remodeling  
502 complexes. *Biochem Cell Biol*. 2009;87(1):35-50.
- 503 51. Biterge B, Schneider R. Histone variants: key players of chromatin. *Cell Tissue Res*. 2014;356(3):457-  
504 466.
- 505 52. Weber CM, Henikoff S. Histone variants: dynamic punctuation in transcription. *Genes Dev*.  
506 2014;28(7):672-682.
- 507 53. Sevilla A, Binda O. Post-translational modifications of the histone variant H2AZ. *Stem Cell Res*.  
508 2014;12(1):289-295.
- 509 54. Hu G, Cui K, Northrup D, et al. H2A.Z facilitates access of active and repressive complexes to chromatin  
510 in embryonic stem cell self-renewal and differentiation. *Cell Stem Cell*. 2013;12(2):180-192.
- 511 55. Ku M, Jaffe JD, Koche RP, et al. H2A.Z landscapes and dual modifications in pluripotent and multipotent  
512 stem cells underlie complex genome regulatory functions. *Genome Biol*. 2012;13(10):R85.
- 513 56. Draker R, Ng MK, Sarcinella E, et al. A combination of H2A.Z and H4 acetylation recruits Brd2 to  
514 chromatin during transcriptional activation. *PLoS Genet*. 2012;8(11):e1003047.
- 515 57. Surface LE, Fields PA, Subramanian V, et al. H2A.Z.1 Monoubiquitylation Antagonizes BRD2 to  
516 Maintain Poised Chromatin in ESCs. *Cell Rep*. 2016;14(5):1142-1155.

517

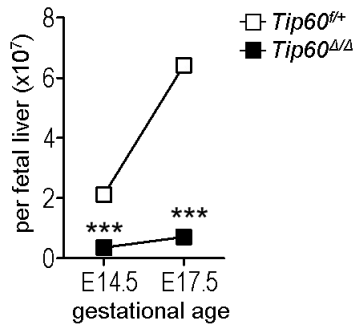
A

Vav-iCre	+	+	-	-	Total
Tip60	f/+	f/f	f/+	f/+	
E11.5	4	6	7	7	24
E14.5	22	18	17	19	76
E17.5	9	7	2	5	23
Weaned	30	0	25	21	76

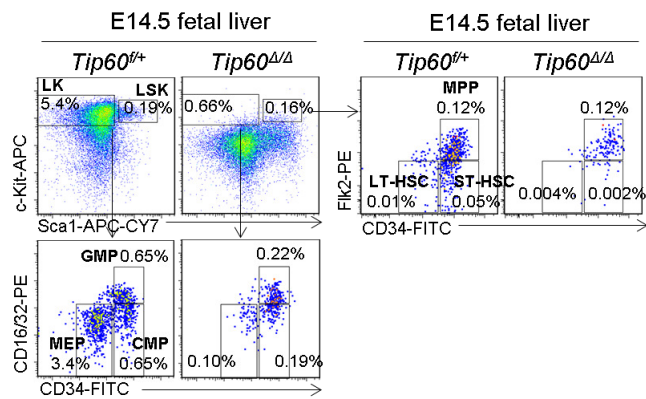
B



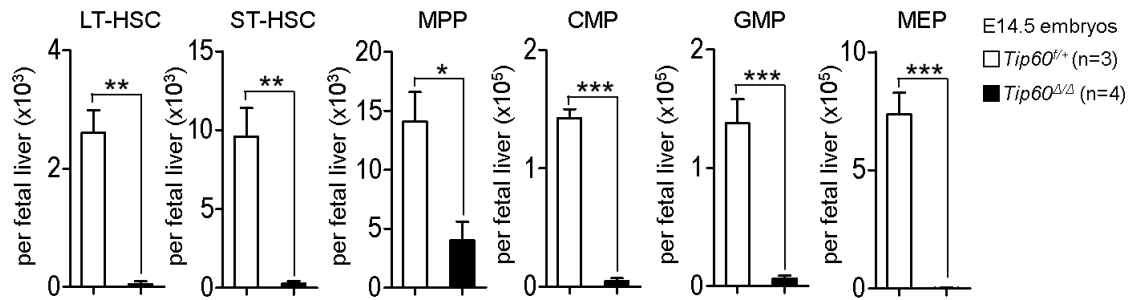
C



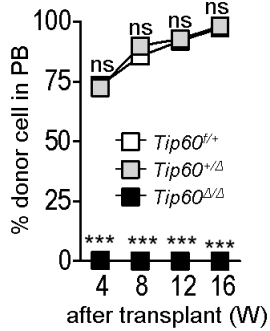
D



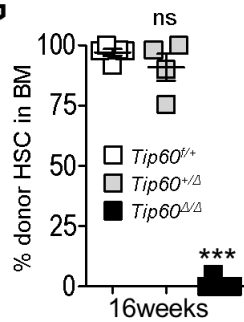
E



F



G

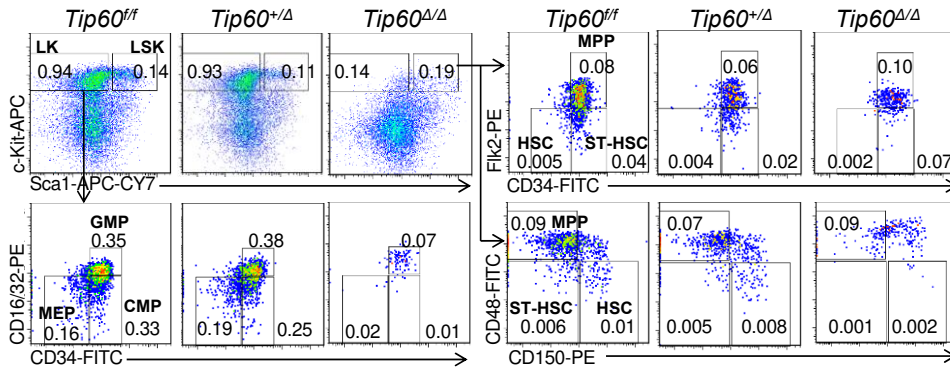


3 **Figure 1. Genetic deletion of *Tip60* leads to fetal hematopoietic failure.**

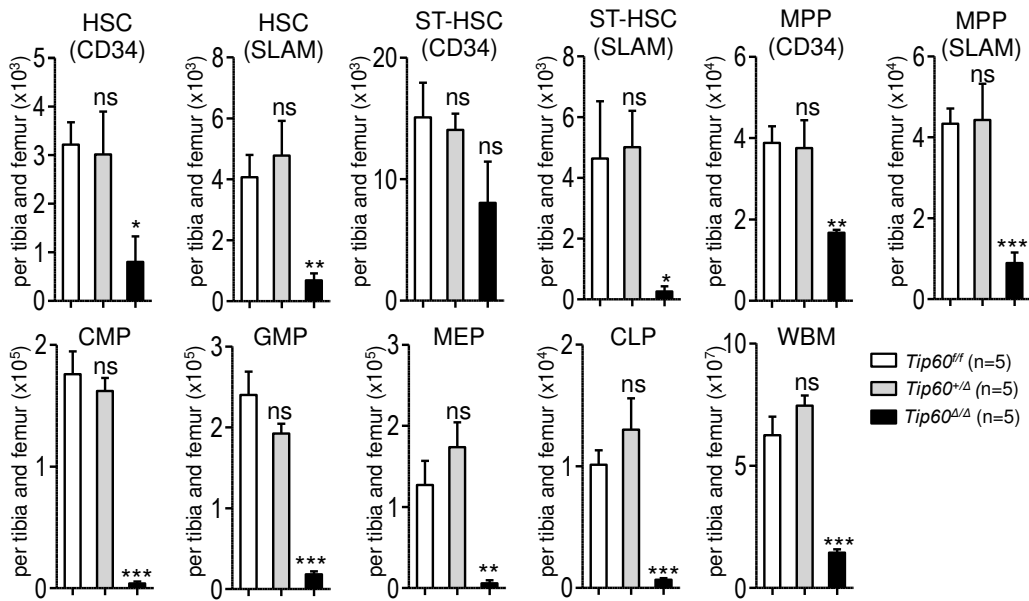
4 **A**, Genotype distribution of offspring and embryos derived from extensive *Tip60<sup>ff</sup> × Tip60<sup>fl+</sup>; Vav-iCre*  
5 breeding. **B**, Representative images of control (*Tip60<sup>fl+</sup>*) and *Tip60<sup>Δ/Δ</sup> (Tip60<sup>ff</sup>; Vav-iCre)* embryo at  
6 E14.5 and E17.5. **C**, Average absolute numbers of nucleated cells from control or *Tip60<sup>Δ/Δ</sup>* fetal liver at  
7 different gestational ages; n = 3–5 embryos for each genotype for each gestational age. **D**,  
8 Representative dot plots of flow cytometry analysis of control and *Tip60<sup>Δ/Δ</sup>* E14.5 fetal liver cells and  
9 frequencies of the gated populations are shown. **E**, Absolute numbers of HSPC subpopulations from  
10 control and *Tip60<sup>Δ/Δ</sup>* E14.5 embryos from the same littermates. LSK (Lin<sup>-</sup>c-Kit<sup>+</sup>Sca-1<sup>+</sup>), LK (Lin<sup>-</sup>c-  
11 Kit<sup>+</sup>Sca-1<sup>-</sup>), LT-HSC (CD34<sup>-</sup>Flk2<sup>-</sup>LSK), ST-HSC (CD34<sup>+</sup>Flk2<sup>-</sup>LSK), MPP (CD34<sup>+</sup>Flk2<sup>-</sup>LSK), GMP  
12 (CD34<sup>+</sup>CD16/32<sup>+</sup>LK), CMP (CD34<sup>+</sup>CD16/32<sup>-</sup>LK), and MEP (CD34<sup>-</sup>CD16/32<sup>-</sup>LK). **F**, 1,000,000 whole  
13 fetal liver cells from control, *Tip60<sup>+/Δ</sup> (Tip60<sup>ff+</sup>; Vav-iCre)*, and *Tip60<sup>Δ/Δ</sup>* E14.5 embryos were  
14 transplanted into lethally irradiated congenic mice (CD45.1<sup>+</sup>) along with 100,000 congenic whole bone  
15 marrow (WBM) (CD45.1<sup>+</sup>CD45.2<sup>+</sup>) cells. Donor chimerism of the recipients' peripheral blood (PB) of  
16 are shown. Statistical analyses were performed versus *Tip60<sup>ff+</sup>* using ANOVA with Bonferroni's post-  
17 test. **G**, Donor chimerism of the recipients' BM HSCs (CD34<sup>+</sup> Flk2<sup>-</sup>LSK) at 16weeks after the  
18 transplantation. The values are presented as mean ± SEM. \*p < 0.05, \*\*p < 0.01, \*\*\*p < 0.001, ns; not  
19 significant.

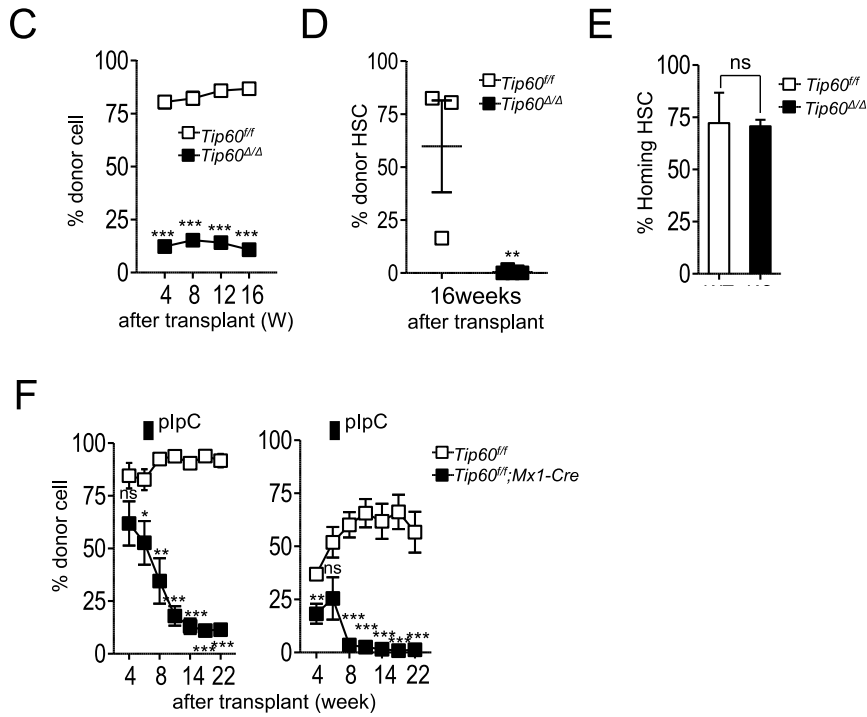


A



B





21

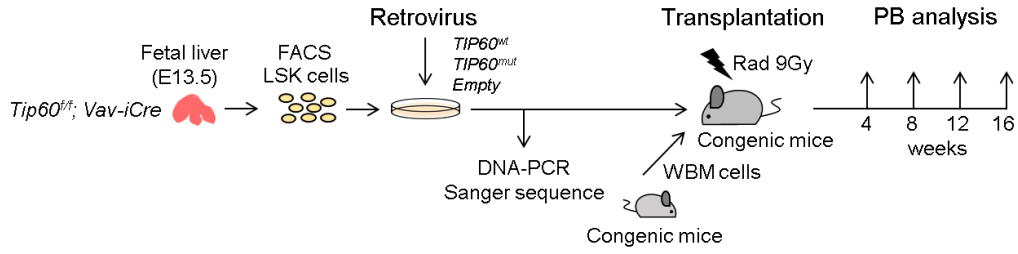
22 **Figure 2. Tip60 is required for adult HSC maintenance in a cell-intrinsic manner.**

23 **A**, 6-10 weeks old, male, *Tip60<sup>fl/fl</sup>*, *Tip60<sup>fl/+</sup>*; *Mx1-Cre* and *Tip60<sup>fl/fl</sup>*; *Mx1-Cre* mice were injected with  
 24 pIpC for 3 consecutive days. BM cells were analyzed for the frequency of HSPCs by flow cytometry 5  
 25 days after the last injection. LSK ( $\text{Lin}^- \text{c-Kit}^+ \text{Sca-1}^+$ ), LK ( $\text{Lin}^- \text{c-Kit}^+ \text{Sca-1}^-$ ), HSC ( $\text{CD34}^+ \text{CD34}^- \text{Flk2}^-$ ;  
 26 SLAM,  $\text{CD150}^+ \text{CD48}^- \text{LSK}$ ), ST-HSC ( $\text{CD34}^+ \text{CD34}^- \text{Flk2}^-$ ; SLAM,  $\text{CD150}^- \text{CD48}^- \text{LSK}$ ), MPP ( $\text{CD34}^+$ ,  
 27  $\text{CD34}^+ \text{Flk2}^+$ ; SLAM,  $\text{CD150}^- \text{CD48}^+ \text{LSK}$ ), GMP ( $\text{CD34}^+ \text{CD16/32}^+ \text{LK}$ ), CMP ( $\text{CD34}^+ \text{CD16/32}^- \text{LK}$ ),  
 28 MEP ( $\text{CD34}^- \text{CD16/32}^- \text{LK}$ ) and CLP ( $\text{Lin}^- \text{IL7R}^+ \text{c-Kit}^+ \text{Sca1}^+ \text{Flk2}^+$ ). Representative dot plots and  
 29 frequencies of HSPC subpopulation from *Tip60<sup>fl/fl</sup>*, *Tip60<sup>+/-</sup>*, and *Tip60<sup>Δ/Δ</sup>* mice are shown. **B**, Absolute  
 30 numbers of HSPCs and WBM cells from *Tip60<sup>fl/fl</sup>*, *Tip60<sup>+/-</sup>*, and *Tip60<sup>Δ/Δ</sup>* mice are shown. **C**,  $1 \times 10^6$   
 31 WBM cells from control *Tip60<sup>fl/fl</sup>* and *Tip60<sup>Δ/Δ</sup>* mice ( $\text{CD45.2}^+$ ) were transplanted into lethally irradiated  
 32 recipient mice ( $\text{CD45.1}^+$ ) along with  $2 \times 10^5$  congenic WBM cells ( $\text{CD45.1}^+ \text{CD45.2}^+$ ). Donor chimerism  
 33 of the recipients' PB are shown. **D**, Donor chimerism of the recipients' BM HSCs ( $\text{CD150}^+ \text{CD48}^- \text{LSK}$ )

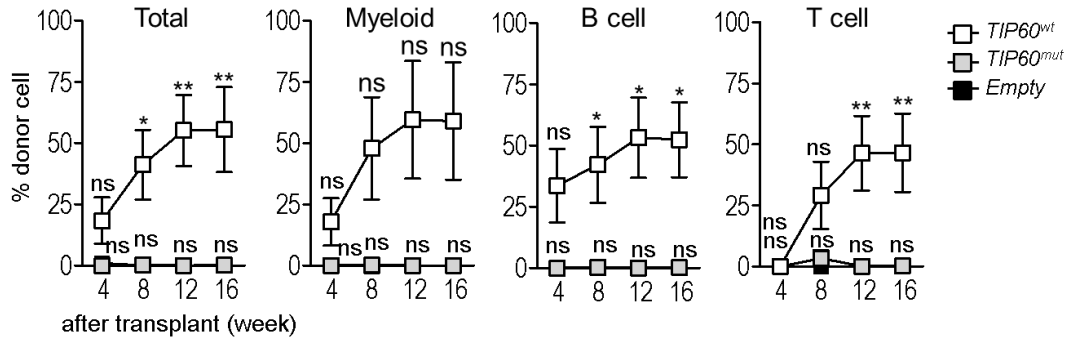
34 at 16 weeks after the transplantation. **E**, CFSE (carboxyfluorescein succinimidyl ester)-labelled HSCs  
35 were injected into lethally irradiated congenic mice and homing efficiency was analyzed 16 hours after  
36 the injection (n=3). **F**, Left,  $1 \times 10^6$  WBM cells from *Tip60<sup>ff</sup>* or *Tip60<sup>ff</sup>; Mx1-Cre* mice (CD45.2<sup>+</sup>) were  
37 transplanted into lethally irradiated recipient mice (CD45.1<sup>+</sup>) along with  $2 \times 10^5$  congenic WBM cells  
38 (CD45.1<sup>+</sup>CD45.2<sup>+</sup>). Right,  $5 \times 10^5$  WBM cells from *Tip60<sup>ff</sup>* or *Tip60<sup>ff</sup>; Mx1-Cre* mice (CD45.2<sup>+</sup>) were  
39 transplanted into lethally irradiated recipient mice (CD45.1<sup>+</sup>) along with  $5 \times 10^5$  congenic WBM cells  
40 (CD45.1<sup>+</sup>CD45.2<sup>+</sup>). pIpC was injected into the recipients 6 weeks after the transplantation. Donor  
41 chimerism in all nucleated cells of the recipients' PB are shown. The values are presented as mean  $\pm$   
42 SEM. \*p < 0.05, \*\*p < 0.01, \*\*\*p < 0.001, ns; not significant.

43

A



B

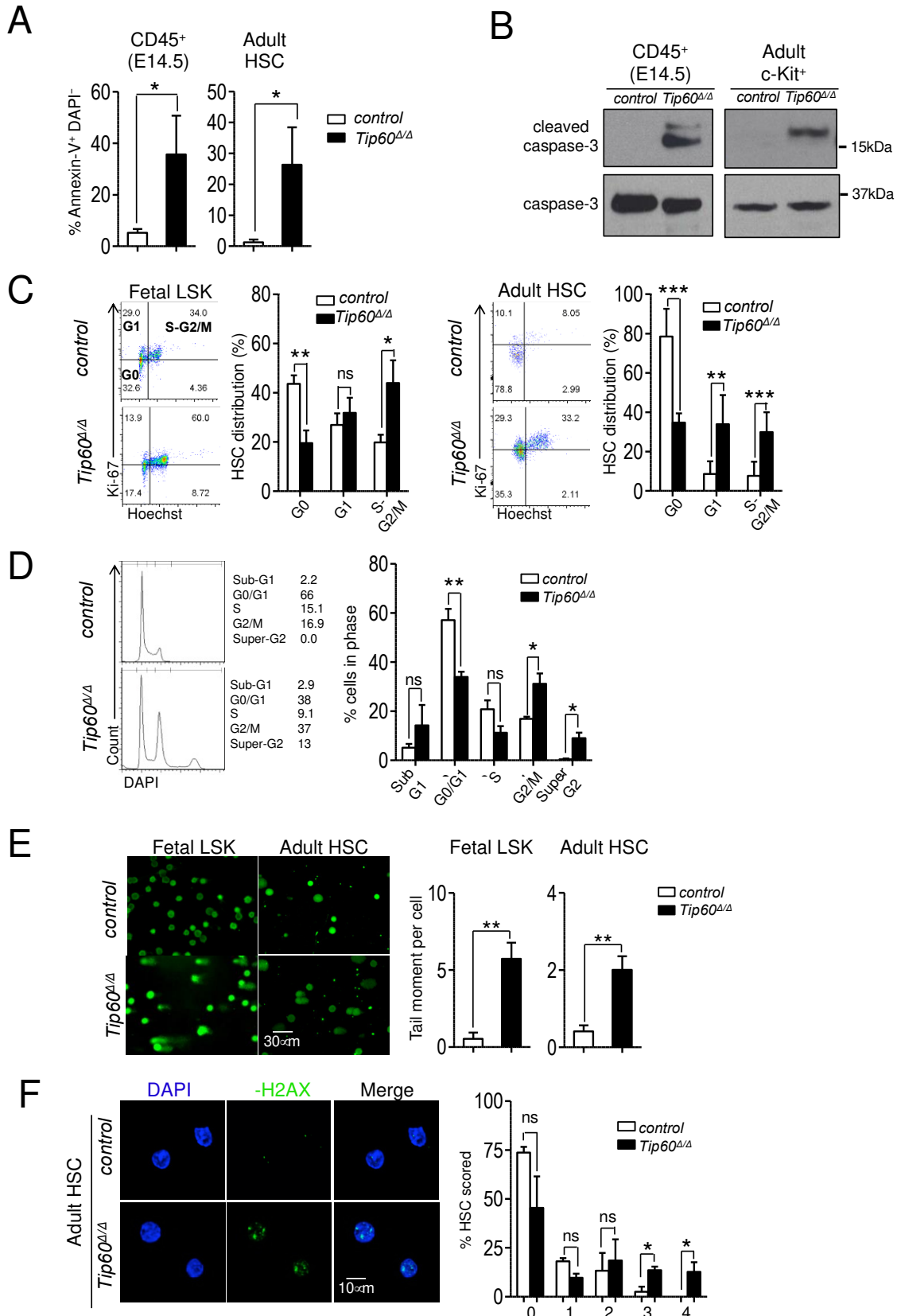


44

45

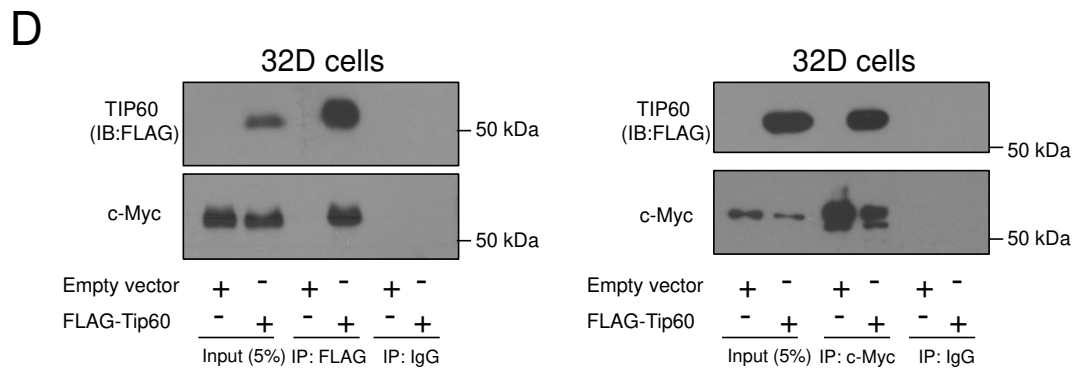
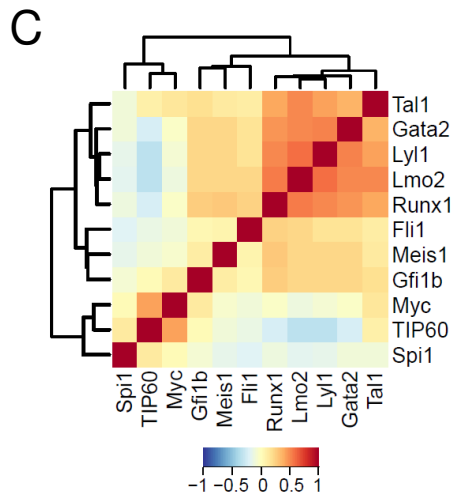
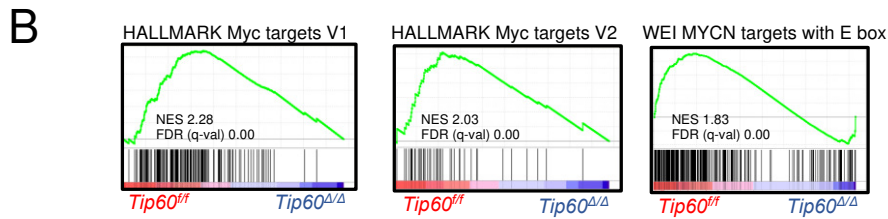
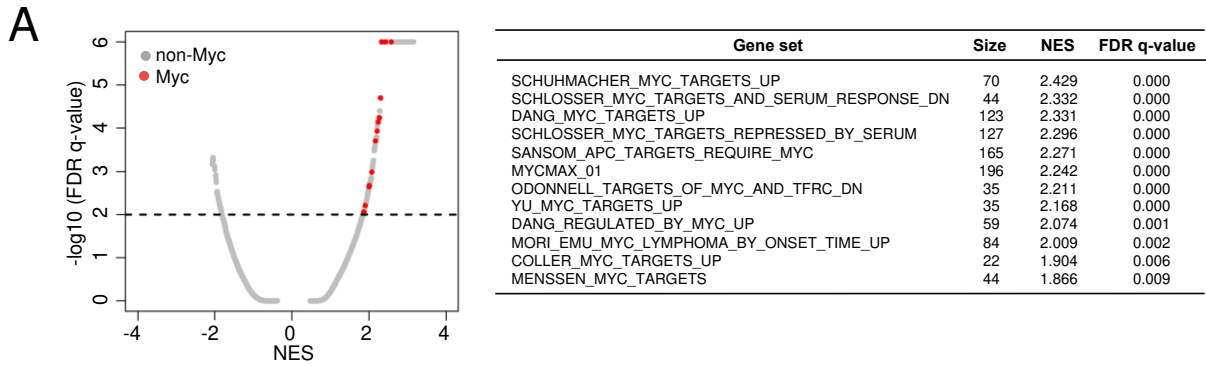
46 **Figure 3. Tip60 acetyltransferase activity is critical for HSC function.**

47 **A**, Experimental scheme for *in vivo* repopulating assays: *Tip60<sup>Δ/Δ</sup>* (*Tip60<sup>fl/fl</sup>*; *Vav-iCre*) LSK cells at E13.5  
48 (CD45.2<sup>+</sup>) were transduced with *TIP60* wild-type (*TIP60<sup>wt</sup>*), catalytically inactive *TIP60* mutant  
49 (*TIP60<sup>mut</sup>*) (Figure S4), and empty vector (Empty) retrovirally, and transplanted into lethally irradiated  
50 recipient mice (CD45.1<sup>+</sup>) along with congenic WBM cells (CD45.1<sup>+</sup>CD45.2<sup>+</sup>). Transduction of plasmid  
51 DNA was verified by Sanger sequencing of the PCR-amplified genomic products. **B**, Chimerism of the  
52 recipients' PB was monitored at different times for 16 weeks after the transplantation. Percentages of  
53 donor cells in total (all nucleated cell), myeloid (Gr1<sup>+</sup>Mac1<sup>+</sup>), B (CD19<sup>+</sup>B220<sup>+</sup>), and T cells  
54 (CD3<sup>+</sup>CD4<sup>+</sup>) of the recipients' PB are shown. The values are presented as mean ± SEM. Statistical  
55 analyses were performed versus *Empty* using ANOVA with Bonferroni's post-test.



2 **Figure 4. Tip60 loss leads to apoptosis and impairs cell cycle progression in HSCs.**

3 **A**, AnnexinV and DAPI staining of CD45<sup>+</sup> cells from E14.5 embryos of control (*Tip60<sup>fl/+</sup>*) (n=3) and  
4 *Tip60<sup>Δ/Δ</sup>* (*Tip60<sup>fl/fl</sup>; Vav-iCre*) (n=4) and BM CD150<sup>+</sup>CD48<sup>-</sup>LSK cells from control (*Tip60<sup>fl/fl</sup>*) (n=3) and  
5 *Tip60<sup>Δ/Δ</sup>* (*Tip60<sup>fl/fl</sup>; Mx1-Cre*) mice (n=3) (pIpC injection on day 1, 2, and 3, and analysis on day 5).  
6 Percentages of AnnexinV<sup>+</sup>DAPI<sup>-</sup> cells are shown. **B**, Immunoblotting of caspase-3 and cleaved caspase-  
7 3 using CD45<sup>+</sup> cells from E14.5 embryos of control and *Tip60<sup>Δ/Δ</sup>* and BM c-Kit<sup>+</sup> cells from control  
8 (*Tip60<sup>fl/+</sup>*) and *Tip60<sup>Δ/Δ</sup>* mice. **C**, Cell-cycle status of fetal LSK (E14.5) (left) and adult  
9 CD150<sup>+</sup>CD48<sup>-</sup>LSK cells (right) were analyzed by flowcytometry. Representative dot plots are shown on  
10 the left, with average percentages of cells in each phase are graphed on the right. **D**, Left, DNA content  
11 analysis by DAPI staining of LSK cells purified from *Tip60<sup>fl/fl</sup>* and *Tip60<sup>fl/fl</sup>; Rosa26-CreERT2* embryos at  
12 E14.5, treated with 4-hydroxytamoxifen (4-OHT) in culture for 5 days. Right, percentages of cells in  
13 each phase are graphed. The values are presented as mean ± SEM. **E**, Assessment of DNA breaks by  
14 alkaline comet assay. Left, images of control (*Tip60<sup>fl/+</sup>*) and *Tip60<sup>Δ/Δ</sup>* fetal LSK cells, and control  
15 (*Tip60<sup>fl/fl</sup>*) and *Tip60<sup>Δ/Δ</sup>* adult CD150<sup>+</sup>CD48<sup>-</sup>LSK cells. Right, quantitative values of tail DNA moment. **F**,  
16 Left, images of immunostaining of γ-H2AX in control (*Tip60<sup>fl/fl</sup>*), and *Tip60<sup>Δ/Δ</sup>* CD150<sup>+</sup>CD48<sup>-</sup>LSK cells.  
17 Right, percentages of cells (Y-axis) which have corresponding number of γ-H2AX foci (X-axis) are  
18 graphed. The values are presented as mean ± SEM. \*p < 0.05, \*\*p < 0.01, \*\*\*p < 0.001, ns; not  
19 significant.

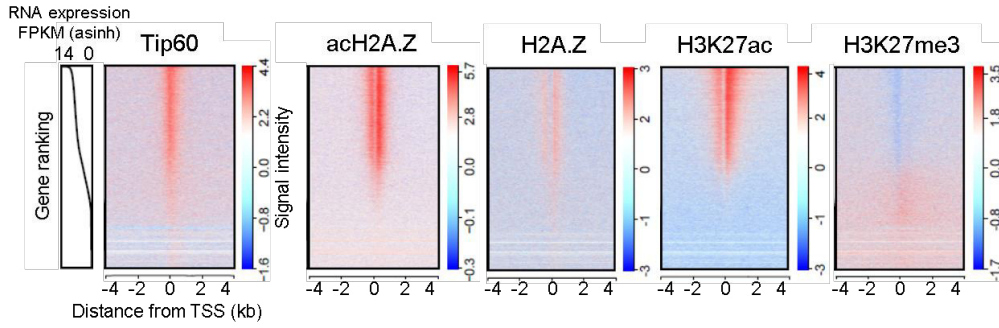




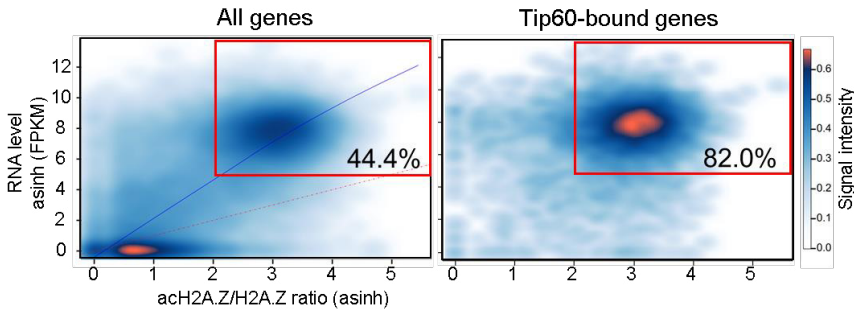
21 **Figure 5. Tip60 regulates Myc target genes.**

22 **A**, Left, a plot of false discovery rate (FDR) versus normalized enrichment score (NES) based on GSEA  
23 from RNA-Seq data of control (*Tip60<sup>f/f</sup>*) versus *Tip60<sup>Δ/Δ</sup>* LSK cells. Distribution of all transcription  
24 factor target gene sets obtained from the MSigDB (c2 and c3) is shown. The red dots indicate the gene  
25 sets for Myc, and the gray for the non-Myc transcription factors. The dashed line represents the FDR  
26 cutoff. Right, list of enriched Myc-associated gene sets. **B**, Representative GSEA plots for Myc target  
27 gene sets. **C**, Correlation analysis of genome-wide occupancy for Tip60 and 10 transcriptional factors  
28 (c-Myc, Tal1, Gata2, Lyl1, Lmo2, Runx1, Fli1, Meis1, Gfi1b, and Spi1) in a murine hematopoietic  
29 progenitor cell line HPC-7 cells, using normalized pointwise mutual information (NPMI). The color  
30 intensity represents the correlation efficiency of each two transcriptional factors. **A total 3651 c-Myc**  
31 **binding peaks, as well as 4347 Tip60, 7596 Tal1, 2796 Gata2, 3432 Lyl1, 5202 Lmo2, 5992 Runx1,**  
32 **18796 Fli1, 7690 Meis1, 3279 Gfi1b, and 18249 Spi1 peaks were identified.** **D**, Left, Hematopoietic  
33 progenitor cells 32D were transduced with FLAG-TIP60. Whole cell lysates were prepared from the  
34 transfected cells and subjected to immunoprecipitation with FLAG-M2 beads. Proteins present in IP or  
35 whole cell lysates (input) were separated by SDS-PAGE and immunoblotted with antibodies for FLAG  
36 and c-Myc. Right, Interaction was confirmed by reciprocal co-IP.

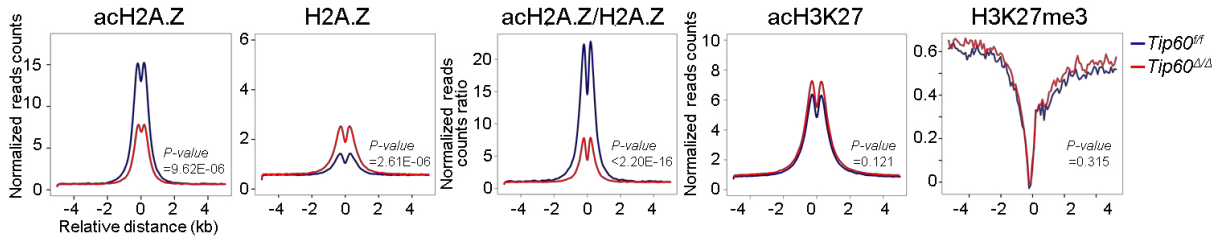
A



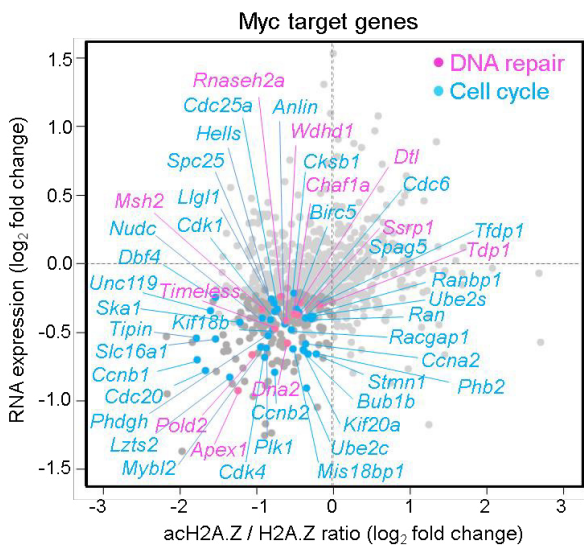
B



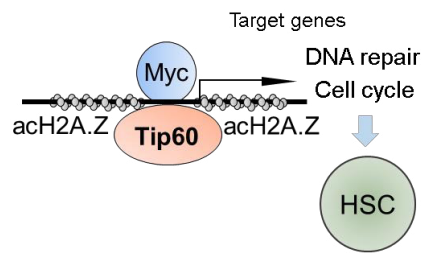
C



D



E



38 **Figure 6. Tip60 maintains the acetylation of H2A.Z to activate Myc target genes.**

39 **A**, An integrated view of Tip60 occupancy and acH2A.Z, H2A.Z, H3K27ac and H3K27me3 enrichment  
40 around transcriptional start sites (TSS  $\pm$  5 kb) in ChIP-seq analysis using wild type fetal c-Kit<sup>+</sup> cells.  
41 Genes were ordered according to the RNA expression levels (line plots) from high (top) to low (bottom).  
42 The color scale represents changes in signal intensity for each antibody. **B**, Cloud plots represent all  
43 (left) and Tip60-bound genes (right) according to the corresponding acH2A.Z/H2A.Z ratio and the RNA  
44 expression level. Correlation analysis between the acH2A.Z/H2A.Z ratio and the RNA expression level  
45 is shown. The blue line represents polynomial regression curve ( $R^2 = 0.7$ ). The red line represents  
46 theoretical linear regression curve ( $Y=X$ ). Genes with high acH2A.Z/H2A.Z ratio ( $> 2$ ) acH2A.Z and  
47 high RNA level ( $\log_2$  FPKM value  $> 5$ ) are squared in red. Tip60 bound genes were identified based on  
48 Tip60 enrichment at the proximal promoter region ( $-1$  kb,  $+100$  bp from TSS). **C**, Mean-plot of  
49 acH2A.Z, H2A.Z, acH2A.Z/H2A.Z ratio, acH3K27 and H3K27me3 enrichment based on relative  
50 distance from Tip60-bound proximal promoter sites in both control (purple) and *Tip60<sup>Δ/Δ</sup>* fetal c-Kit<sup>+</sup>  
51 cells (red). Statistical analyses were performed using Mann-Whitney-Wilcoxon method. **D**, 816 Myc  
52 target genes were identified to be transcribed in both control and *Tip60<sup>Δ/Δ</sup>* fetal LSK cells in the RNA-  
53 seq analysis. X-axis indicates  $\log_2$  fold change in acH2A.Z/H2A.Z ratio at TSS ( $\pm 1$ kb) induced by *Tip60*  
54 deletion and Y-axis indicates  $\log_2$  fold change in RNA expression level. DNA repair related genes (blue)  
55 and cell-cycle related genes (pink) with significant downregulation in their RNA levels ( $p < 0.05$ ) are  
56 labelled. Myc target genes are obtained from the gene sets described in [Figure 5A](#). DNA repair and cell-  
57 cycle related genes belong to Gene Ontology category GO:0006281 and GO:0007049, respectively. **E**,  
58 Tip60 maintains HSC thorough acetylation of H2A.Z to activate Myc target genes, regulating cell-cycle  
59 and DNA repair processes.